Chinese Journal of
POLYMER SCIENCE

RESEARCH ARTICLE

https://doi.org/10.1007/s10118-024-3225-2
Chinese J. Polym. Sci. **2024**, *42*, 1888–1896

Vinylic-addition Polynorbornene-based Anion-Exchange Membranes with Semi-Interpenetrating Polymer Networks for Water Electrolysis

Ting Wang[a,b], Yu Wang[a*], and Wei You[a,b*]

[a] *Beijing National Laboratory for Molecular Sciences (BNLMS), CAS Key Laboratory of Engineering Plastics, Institute of Chemistry, Chinese Academy of Sciences, Beijing 100190, China*
[b] *University of Chinese Academy of Sciences, Beijing 100049, China*

Electronic Supplementary Information

Abstract Anion-exchange membranes (AEMs) with high conductivity and stability are essential components of hydrogen related water electrolysis and fuel cell applications. During the past decades, polynorbornene (PNB)-based AEMs have shown excellent performance due to their saturated all-carbon-based backbones and diverse strategies to prepare cross-linked membranes. However, nearly all previously reported PNB-based AEMs rely on the alkyl-substituted norbornene monomers, whose low-yielding synthesis leads to high-cost of the AEMs. In addition, the cross-linked PNB-based AEMs usually suffered from mechanical brittleness. Herein, we propose a novel semi-interpenetrating polymer network (s-IPN) strategy to simultaneously enhance mechanical modulus and ionic conductivity, while using commercial 5-vinyl-2-norbornene (VNB) as the single norbornene derivatives to prepare high-performance AEMs. A diallylphenol quaternary ammonium salt was used for photo-induced cross-linking with poly-VNB and various dithiols to produce AEMs with s-IPN structures. The resultant membranes have excellent hydroxide conductivities and alkaline stability in 1 mol/L KOH at 80 °C, and are successfully applied in alkaline anion-exchange membrane water electrolyzers to stably operate for over 150 h.

Keywords Anion-exchange membranes; Semi-interpenetrating polymer network; Vinylic-addition polynorbornene; Thiol-ene click reaction; Alkaline water electrolysis

Citation: Wang, T.; Wang, Y.; You, W. Vinylic-addition polynorbornene-based anion-exchange membranes with semi-interpenetrating polymer networks for water electrolysis. *Chinese J. Polym. Sci.* **2024**, *42*, 1888–1896.

INTRODUCTION

Hydrogen is an attractive and ecologically clean energy, and its combustion product is water.[1–3] In recent years, the "green hydrogen" from water electrolysis has received extensive attention. Traditional water electrolysis processes can be divided into two categories: alkaline water electrolysis (AWE) and proton-exchange membrane water electrolysis (PEMWE).[1,4] Although AWE has the advantage of low-cost, the high concentration of KOH electrolyte carries the risk of corrosion of the equipment. Furthermore, the porous separator used to isolate the anode and cathode in AWE prevents the generation of pressurized hydrogen.[5] The above disadvantages lead to AWE suffer from low efficiency and safety concerns. On the other hand, PEMWE is a zero-gap configuration that can reduce AWE internal resistance. Therefore, PEMWE can improve current density and generate high-pressure hydrogen. However, the acidic conditions in which PEM operates result in the use of expensive membranes (such as Nafion), electrocatalysts (such as Ir and Pt), and bipolar plates.[5,6] For improving the efficiency of water electrolysis, anion-exchange membrane water electrolysis (AEMWE) has been developed and has received a great attention in recent years. AEMWE operates in alkaline environment, and the zero-gap configuration involved in AEMWE allows it to exempt from the use of precious metal catalysts and exhibits fast cathodic reaction kinetics.[5,7–9] Therefore, AEMWE has become an attractive green method for hydrogen production.

The anion-exchange membrane (AEM), as a critical component of AEMWE, is consisted of polymeric backbones, cations attached to the backbone *via* covalent bonds, and free anions.[9] The conductivity and dimensional/mechanical/alkaline stabilities of AEMs are considered to be the important factors to enhance the current density and durability of AEMWE devices. However, the conductivity and alkaline stability have become great challenges in the development of AEMs.[10–12] A high ion exchange capacity (IEC) is required to achieve the high conductivity for AEMs, but lead to an excessive swelling, thereby reducing the stability of AEMs.[13–15] To improve the stability or comprehensive performance of AEMs, several strategies have been proposed, including the use of alkali resistant aromatic ether free polymer backbone structures,[16–24] the introduction of alkaline stable cationic

* Corresponding authors, E-mail: ywang507@iccas.ac.cn (Y.W.)
E-mail: weiyou@iccas.ac.cn (W.Y.)

Received August 3, 2024; Accepted September 5, 2024; Published online November 7, 2024

groups,[25–28] the construction of microphase separation to provide ion transport channels,[29–33] and cross-linking/blending strategies.[34–37] The cross-linking strategy has been proven to effectively enhance the mechanical strength and dimensional stability of AEMs. However, cross-linking usually compromises with a decrease in conductivity. Interpenetrating polymer network (IPN) and semi-interpenetrating polymer network (s-IPN) are novel approaches to enhance mechanical modulus and ionic conductivity simultaneously, which can effectively address the trade-off between conductivity and stability.[38,39] IPN is a polymer mixture composed of two or more interpenetrating polymer networks, and if only one polymer in the polymer mixture forms cross-linked networks, it is called s-IPN.[39] Wei *et al.*[39] reported IPN AEMs consisted of cross-linked quaternized poly(vinylbenzyl chloride) (PVBC) and cross-linked poly(vinyl alcohol) (PVA) for H_2/air (CO_2-free) alkaline fuel cell. They also reported[40] dual-cation IPN AEMs with cross-linked quaternized poly(2,6-dimethyl-1,4-phenylene oxide) (QPPO) and cross-linked quaternized PVBC, which increased the IEC and OH^- conductivity. Zhuang *et al.* [41] synthesized transparent s-IPN AEMs composed of cation cross-linked polystyrene-*b*-poly(ethylene-*co*-butylene)-*b*-polystyrene (SEBS) and highly charged QPPO. Alkali-resistant SEBS enhanced dimensional stability and chemical stability of the s-IPN AEMs. Li *et al.*[42] reported s-IPN AEMs composed of quaternized poly(styrene) (PS) and cross-linked poly(2,6-dimethyl-1,4phenylene oxide) (PPO).

For the reported IPN and s-IPN AEMs, most of them focused on the aromatic-containing backbones such as PPO, PS, SEBS, PVBC, but the aromatic groups are reported to have issues of low oxidative stability and easy electrocatalyst adsorption.[43] Among AEMs with heteroatom-free backbones, vinylic-addition polynorbornenes (PNBs) possess excellent thermal and chemical stability as well as good film-forming properties,[22,23] yet have not been utilized to build IPN or s-IPN systems. More importantly, in order to incorporate cationic functional groups in PNBs, nearly all previous reports rely on the use of alkyl-substituted norbornene,[44–46] which suffered from low yielding monomer synthesis and thus high cost of the membranes. More recently, Zhuang *et al.*[47] reported a novel strategy using the homopolymer of poly(5-vinyl-2-norbornene) (PVNB), and the cationic groups were connected through a Ru-catalyzed cross-metathesis post-polymerization functionalization to prepare high-performance AEMs. Herein, we prepared a series of vinylic-addition polynorbornene-based s-IPN AEMs with PVNB as the mechanical support phase and diallylphenol quaternary ammonium salt as the ion conduction phase. Cross-linking with various dithiols gave rise to s-IPN AEMs under UV irradiation by thiol-ene click reactions. The PVNB was prepared from the homopolymerization of commercial VNB monomers. The use of quaternary ammonium cationic monomer enabled the preparation of AEMs without the need for post-polymerization quaternization. This convenient s-IPN strategy results in AEMs with excellent hydroxide conductivities, good thermal and alkaline stability, low water absorption, and low swelling ratios.

EXPERIMENTAL

The synthetic details, experimental section and complementary data are presented in the electronic supplementary information (ESI).

RESULTS AND DISCUSSION

PVNB was prepared according to our previous reports.[22,23] We used the three-component catalytic system (tris(dibenzylideneacetone) dipalladium ($Pd_2(dba)_3$), tricyclohexyl phosphine (PCy_3), and lithium ion diethyl ether tetrakis(pentafluorophenyl)-boranuide (Li[FABA])) to synthesize vinylic-addition polymer of VNB. The number average molecular weights (M_n) and polydispersity ($Đ$) of the resulting vinylic-addition polynorbornene was determined by gel permeation chromatography (GPC) to be 37.5 kDa and 2.38, respectively (Fig. S1 in ESI). Two types of 2,6-diallylphenol quaternary ammonium salt monomers with trimethylammonium cation and piperidinium cation (3 and 5) were synthesized by nucleophilic reaction of 2,6-diallylphenol (1) and monobromo quaternary ammonium salt (2 and 4) (Scheme 1). The proton nuclear magnetic resonance (^{1}H-NMR) spectra of polymer VA-PNB, intermediate product 2,6-diallylphenol (1), and monomer 2,6-diallylphenol quaternary ammonium salt (3 and 5) are shown in Figs. S2–S5 (in ESI).

Semi-interpenetrating polymer network (s-IPN) AEMs were prepared by the thiol-ene click reactions under UV irradiation (Scheme 2). First, polymer PVNB was dissolved in trichloromethane at room temperature. Then the corresponding 2,6-diallylphenol quaternary ammonium salt, dithiol, and photo-initiator (phenylbis(2,4,6-trimethylbenzoyl)phosphine oxide) were added. The obtained solution was poured into a mold, and the cross-linking reaction was carried out with simultaneous solvent evaporation under UV irradiation (365 nm) for 30 min to obtain the cross-linked s-IPN membranes in the Br^- form. The membranes were denoted as ***x-y-z*** followed by the types of thiols and cations, where ***x***, ***y***, ***z*** represent the equivalent ratio of alkenes in PVNB, 2,6-diallylphenol quaternary ammonium salt, and dithiol, respectively. **C6OSH, C6SH, C8SH**, and **ArSH** represent using the 3,6-dioxa-1,8-octanedithiol, 1,6-hexanedithiol, 1,8-octanedithiol, and 1,4-benzenedithiol as the cross-linking agents, respectively (Scheme 2). **TMA** and **PIP** represent the trimethylammonium and piperidinium cation, respectively. Except for **ArSH**, which a free-standing film could not be obtained, all other dithiols gave rise to mechanically intact, smooth, and transparent membranes (such as the picture in Fig. S6 in ESI). As a control sample, the membranes obtained by casting a solution of 2,6-diallylphenol quaternary ammonium salt, dithiol, and photoinitiator under UV irradiation without the addition of PVNB were extremely inhomogeneous and fragile, confirming the importance of PVNB as the mechanical support.

The detailed properties of the s-IPN AEMs are listed in Table 1. The IEC values of AEMs obtained by theoretical calculation and Mohr titration were found to be close. For **1.0-0.25-0.5 C6OSH TMA** membrane, the low IEC and conductivity result from the low proportion of diallyl quaternary ammonium salt cations involved. When the amount of quaternary ammonium cations increased, the IEC and conductivity of membrane **0.6-0.4-0.5 C6OSH TMA** increased, but at the same time the water absorption increased to 99%. In order to regulate the water uptake of the membranes, we attempted to vary the type of dithiols, using full carbon backbone 1,6-hexanedithiol and 1,8-octanedithiol, both of which yielded

https://doi.org/10.1007/s10118-024-3225-2

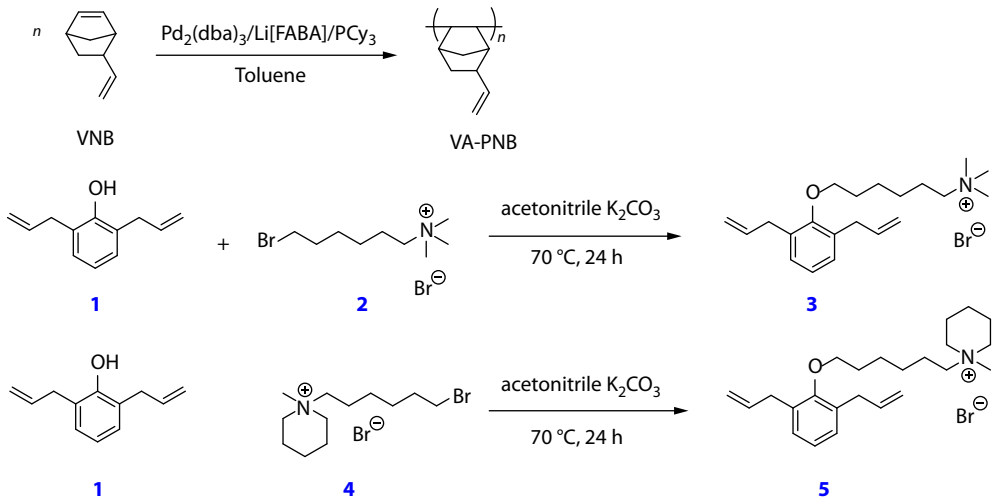

Scheme 1 Synthesis of the vinylic addition polynorbornene and diallylphenol quaternary ammonium salt.

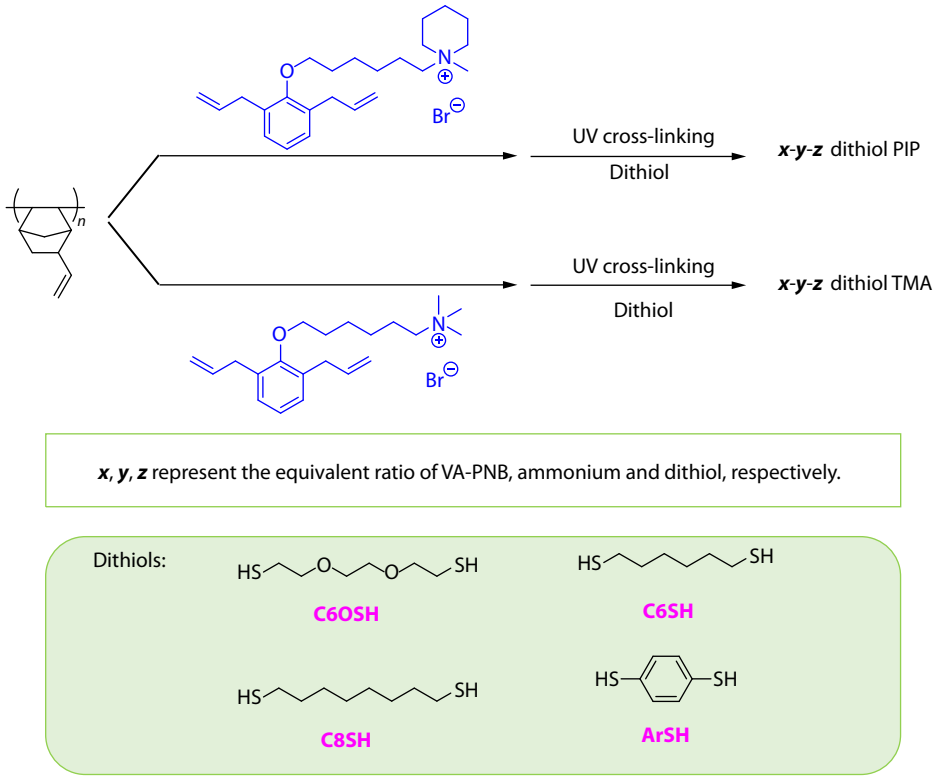

Scheme 2 Preparation of vinylic-addition polynorbornene-based semi-interpenetrating polymer network anion exchange membranes.

Table 1 Detailed properties of the dithiol-cross-linked VA-PNB-AEMs.

Membranes	IEC [a] (mmol Cl^-/g)	IEC [b] (mmol Cl^-/g)	σ (HCO_3^-, 25 °C) (mS/cm)	WU [c] (%)
1.0-0.25-0.5 C6OSH TMA	0.79	0.67±0.04	2.1±0.1	23
0.6-0.4-0.5 C6OSH TMA	1.20	1.18±0.01	5.9±0.1	99
0.6-0.4-0.5 C6SH TMA	1.27	1.30±0.02	7.8±0.1	39
0.5-0.4-0.45 C6SH TMA	1.35	1.43±0.02	8.1±0.1	66
0.6-0.4-0.5 C6SH PIP	1.21	1.18±0.03	5.5±0.2	21
0.6-0.4-0.5 C8SH TMA	1.21	1.23±0.02	6.7±0.2	35

[a] The theoretical ion exchange capacity (IEC) was calculated from the feed ratio (including the mass of the dithiol); [b] IEC was determined by Mohr titration. The conductivities and IECs were obtained according to the average of three samples; [c] WU was determined with samples in the HCO_3^- form at 25 °C.

https://doi.org/10.1007/s10118-024-3225-2

AEMs (**0.6-0.4-0.5 C6SH TMA, 0.6-0.4-0.5 C8SH TMA**) with reduced water uptake. With a further increase in diallyl quaternary ammonium salt cation content and the use of 1,6-hexanedithiol as the cross-linking agent, the **0.5-0.4-0.45 C6SH TMA** membrane exhibited higher IEC and conductivity with appropriate water absorption. When the cation was changed to piperidine cation, the conductivity of **0.6-0.4-0.5 C6SH PIP** membrane was slightly lower than that of the corresponding trimethylamine cation at the same content (**0.6-0.4-0.5 C6SH TMA**).

The high hydroxide conductivity of the AEM is a crucial property, which was desired to improve the current density of AEMWE. The "true hydroxide conductivities" of the s-IPN AEMs were measured using an *in situ* de-carbonation protocol under direct current and high humidity conditions (relative humidity (RH) > 98%, Fig. 1).[48,49] The results showed that the hydroxide conductivities of all membranes increased with temperatures. **0.6-0.4-0.5 C6SH TMA** membrane exhibited significantly higher hydroxide conductivities compared to **0.6-0.4-0.5 C6SH PIP** membrane. The hydroxide conductivity of **0.6-0.4-0.5 C6SH TMA** membrane was up to 120 mS/cm at 90 °C. Under the same feeding ratio, the conductivities of AEMs obtained by using 1,6-hexanedithiol as the cross-linking agent is optimal (Fig. 1a). The Arrhenius plots of the hydroxide conduction indicated that the apparent activation energy values (E_a) were within the range of 8.3–12.1 kJ/mol (Fig. 1b and Table S1 in ESI), which were similar to the previously reported cross-linked VA-PNB-AEMs.[44]

The appropriate amount of water is necessary for ion hydration and conductivity, while over-swelling can be a critical issue for AEMs due to mechanical failure. The WU and SR of the **0.6-0.4-0.5 C6SH TMA** and **0.6-0.4-0.5 C6SH PIP** membranes at different temperatures are shown in Figs. 2(a) and 2(b), respectively. The membranes remained low WU and SR even at high temperatures (with WU less than 50% and SR less than 12% at 80 °C). This was attributed to the cross-linking effect of dithiols and the formation of s-IPN, which helped maintaining the dimensional stability and integrity of the membranes. No evident peaks were observed in the small-angle X-ray scattering (SAXS) results (Fig. S7 in ESI) of **0.6-0.4-0.5 C6SH TMA** and **0.6-0.4-0.5 C6SH PIP** membranes.[22,23] By the SAXS results, the microstructures of s-IPN were likely dominated by the cross-linking in this work, which inhibits the formation of microphase-separated structures while improving the mechanical properties.

Thermogravimetric analyses (TGA) were performed to eval-

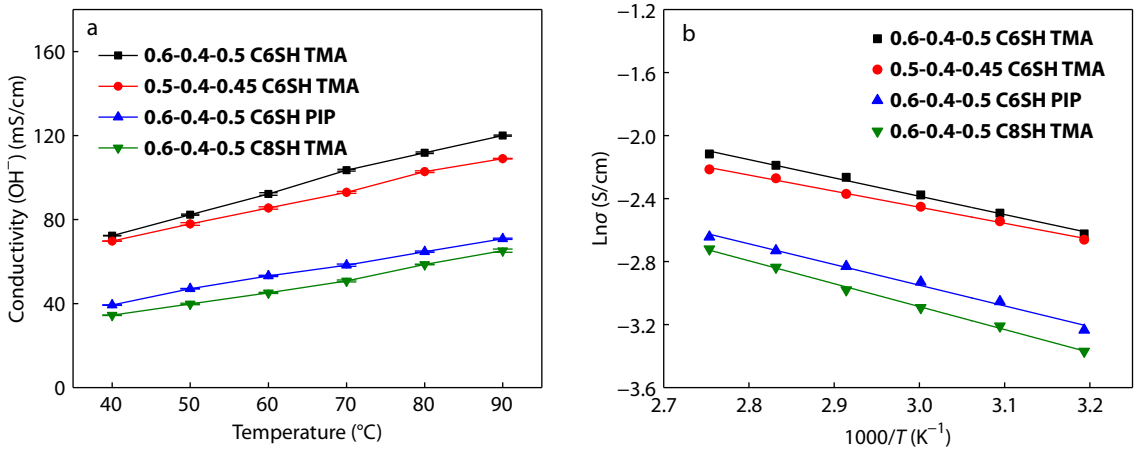

Fig. 1 Temperature dependence of: (a) Hydroxide conductivities for the s-IPN membranes with different salt cations; (b) Arrhenius plots of the samples.

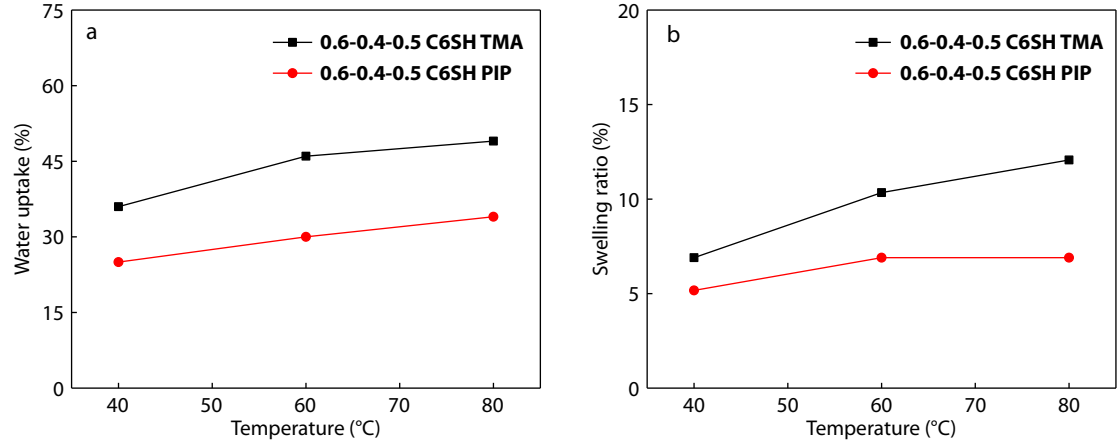

Fig. 2 (a) Water uptake and (b) swelling ratio of **0.6-0.4-0.5 C6SH TMA** and **0.6-0.4-0.5 C6SH PIP** membranes with HCO_3^- counter-anions at various temperatures.

https://doi.org/10.1007/s10118-024-3225-2

uate the thermal stability of **0.6-0.4-0.5 C6SH TMA** and **0.6-0.4-0.5 C6SH PIP** membranes. The TGA results and the derivative thermogravimetry (DTG) curves are shown in Fig. 3. There are three mass-loss stages in the TGA thermogram: the first stage at about 250 °C corresponds to the loss of the quaternary ammonium groups;[50,51] the second stage of degradation around 350 °C is possibly attributed to the linkers and sulfur-based cross-linkers within the AEMs; and the third mass loss at over 400 °C is derived from polymer backbone decomposition. These curves indicate that all the membranes exhibited no significant degradation below 200 °C, suggesting that they possess excellent thermal stability that meet the required operating temperature range of AEMWE (60–80 °C). The mechanical properties of the AEMs were evaluated by tensile measurements. The stress-strain curves of **0.6-0.4-0.5 C6SH TMA** and **0.6-0.4-0.5 C6SH PIP** membranes are shown in Fig. S8 (in ESI). The stress-at-break of **0.6-0.4-0.5 C6SH TMA** membrane is 30±1 MPa, which is higher than that of **0.6-0.4-0.5 C6SH PIP** membrane. However, the strain-at-break of **0.6-0.4-0.5 C6SH PIP** membrane is 40%±2%, which is higher than that of **0.6-0.4-0.5 C6SH TMA** membrane. The temperature dependence of the storage modulus (E'), which represents the ability to resist deformation for the membranes, was found to be similar for **0.6-0.4-0.5 C6SH PIP** and **0.6-0.4-0.5 C6SH TMA** through the DMA measurements (Fig. 4). The T_g of **0.6-0.4-0.5 C6SH PIP** above which the molecular chains between the cross-linking points begin to long-range coordinated motion was determined to be *ca.* 100.4 °C by the peak temperature of the tanδ (=E''/E', where E'' is the loss modulus), higher than that of **0.6-0.4-0.5 C6SH TMA** (Fig. 4b). Under the same feeding ratio, the types of cations are affecting the mechanical properties of the s-IPN AEMs, possibly due to different strength of ionic interactions.[52–55]

The alkaline stability of the AEMs is critical for their effective use in AEMWE, which can directly affect the durability of device. The alkaline stabilities of **0.6-0.4-0.5 C6SH TMA** and **0.6-0.4-0.5 C6SH PIP** membranes were evaluated by soaking them in a 1 mol/L KOH solution at 80 °C for 35 days. The bicarbonate conductivities of the membranes were measured every five days, and the results showed that both membranes exhibited good alkaline stability, with 73% and 86% conductivity remaining after 35 days for **0.6-0.4-0.5 C6SH TMA** and **0.6-0.4-0.5 C6SH PIP** membranes, respectively (Fig. 5a). By measuring the IEC change of the membranes before and after the alkaline stability testing, it was found that 85% and 91% IEC were remained for **0.6-0.4-0.5 C6SH TMA** and **0.6-0.4-0.5 C6SH PIP** membranes, respectively (Fig. 5b). The FT-IR analysis on the membranes before and after the alkaline sta-

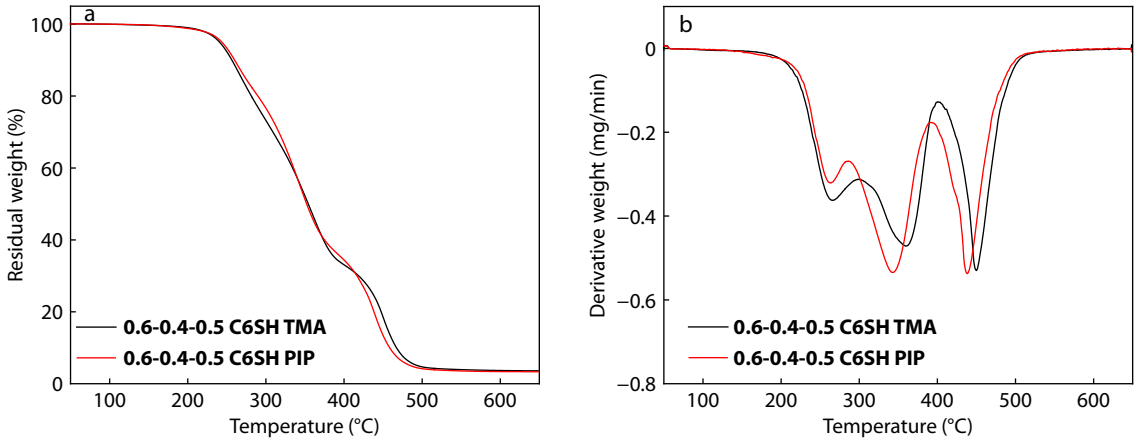

Fig. 3 (a) TGA curves and (b) DTG curves of **0.6-0.4-0.5 C6SH TMA** and **0.6-0.4-0.5 C6SH PIP** membranes with Br counter-anions.

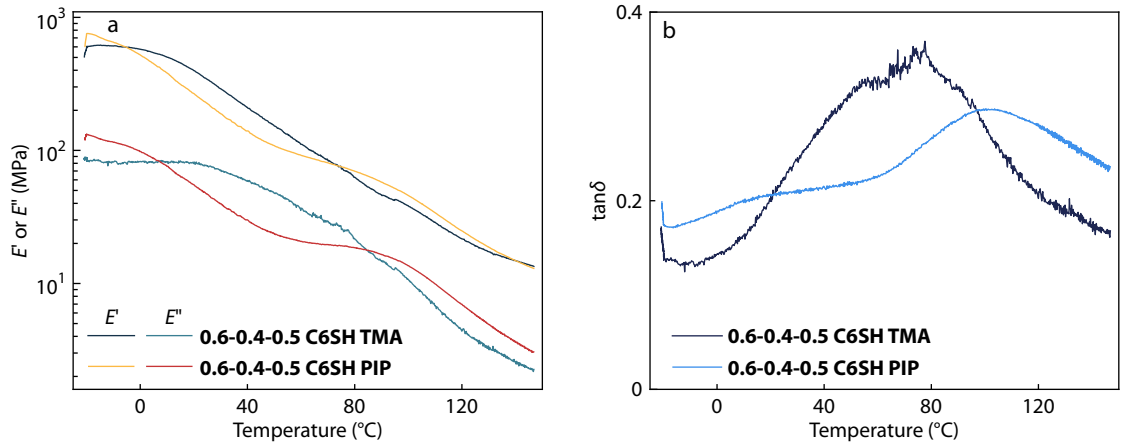

Fig. 4 Temperature dependence of (a) storage and loss moduli, and (b) tanδ of **0.6-0.4-0.5 C6SH TMA** and **0.6-0.4-0.5 C6SH PIP** membranes.

https://doi.org/10.1007/s10118-024-3225-2

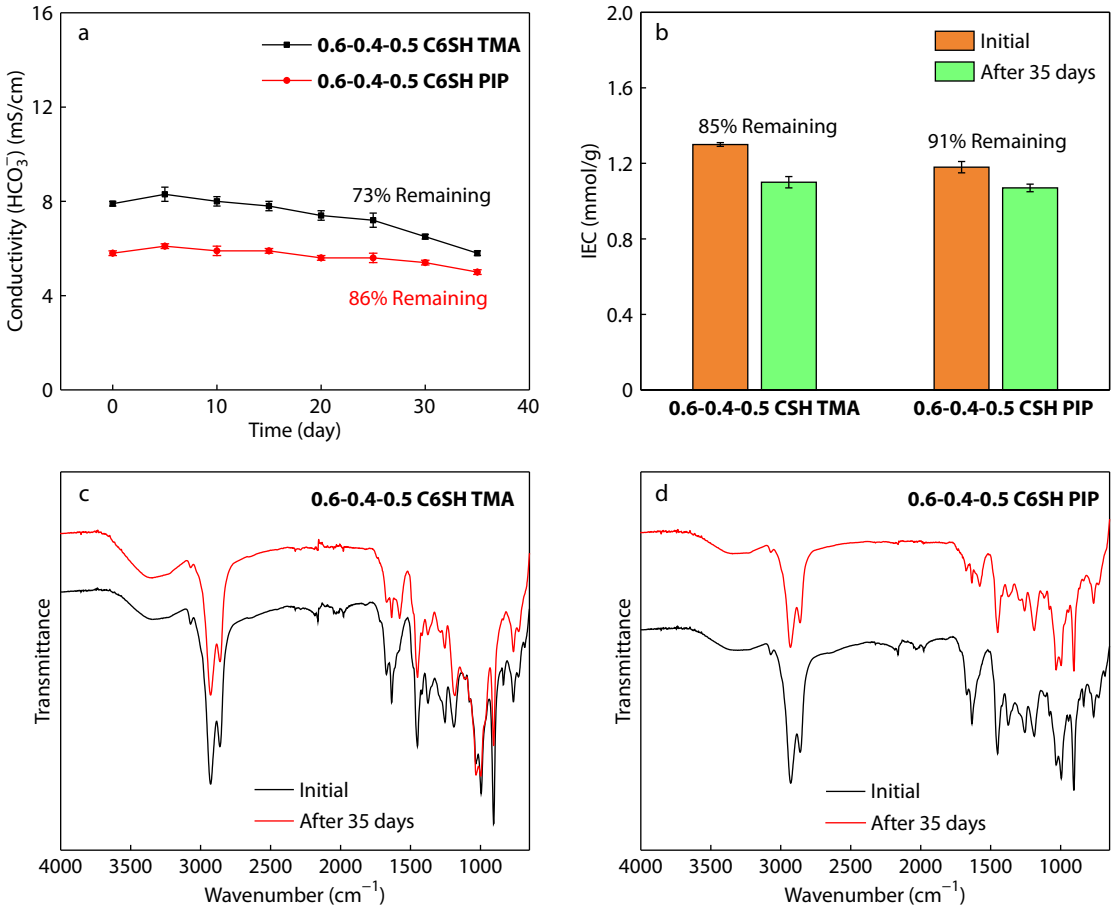

Fig. 5 (a) Conductivity stability test of **0.6-0.4-0.5 C6SH TMA** and **0.6-0.4-0.5 C6SH PIP** membranes in 1 mol/L aqueous KOH solution at 80 °C; (b) The changes in IEC of **0.6-0.4-0.5 C6SH TMA** and **0.6-0.4-0.5 C6SH PIP** membranes in 1 mol/L aqueous KOH solution at 80 °C for 35 days; (c) The FT-IR spectra of **0.6-0.4-0.5 C6SH TMA** membrane before and after in 1 mol/L aqueous KOH solution at 80 °C for 35 days; (d) The FTIR spectra of **0.6-0.4-0.5 C6SH PIP** membrane before and after in 1 mol/L aqueous KOH solution at 80 °C for 35 days.

bility testing revealed that the basic structure of the membranes was not significantly influenced (Figs. 5c and 5d).[23] This suggests that the cation degradation is likely the primary factor affecting alkaline stability of the AEMs.

The membranes **0.6-0.4-0.5 C6SH TMA** and **0.6-0.4-0.5 C6SH PIP** were subjected to AEMWE assembly for device performance evaluation. We utilized the catalyst-coated substrate (CCS) method to fabricate the membrane electrode assemblies (MEAs). For the anode, precious metal catalyst IrO_2 and non-precious metal catalysts Ni_2Fe_1 and $NiFe_2O_4$ on stainless steel, respectively. For the cathode, precious metal catalyst Pt/Ru/C on carbon and non-precious metal catalyst NiFeCo on Ni fiber mat, respectively. Fig. 6(a) shows the polarization curves of **0.6-0.4-0.5 C6SH TMA** and **0.6-0.4-0.5 C6SH PIP** measured in 1 mol/L KOH at 60 °C when using IrO_2 and Pt/Ru/C as catalysts. At an applied cell voltage of 2.0 V, the MEAs achieved electrolytic currents of 534 and 193 mA·cm^{-2} for **0.6-0.4-0.5 C6SH TMA** and **0.6-0.4-0.5 C6SH PIP**, respectively. The current density of AEMWE assembled with TMA cation-containing membranes was significantly higher than that of AEMWE assembled with PIP cation-containing membranes, which was attributed to the higher conductivity of the former, as shown in Fig. 1(a). When changing the concentration of the electrolyte (the KOH concentration was reduced to 0.1 mol/L or replace the electrolyte with pure water) or the operating temperature (40–80 °C) of the AEMWE, the MEAs could still operate smoothly (Figs. S9 and S10 in ESI). When the catalyst for the anode is replaced by a non-precious metal catalyst Ni_2Fe_1 and the cathode is still using Pt/Ru/C, the current density of the MEA assembled with **0.6-0.4-0.5 C6SH TMA** is slightly reduced and the polarization curve does not change much (Fig. 6b). It is worth mentioning that when non-precious metal catalysts NiFeCo and $NiFe_2O_4$ were used at the cathode and anode, respectively, the current density of the MEA assembled with **0.6-0.4-0.5 C6SH TMA** is even increased above 2 V compared to the precious metal catalysts. Durability tests of AEMWE were conducted with 1 mol/L KOH electrolyte at 60 °C under constant current mode of 500 mA·cm^{-2} (Fig. 7). The AEMWE for **0.6-0.4-0.5 C6SH TMA** assembled MEA exhibited stable operation for more than 150 hours with IrO_2 and Pt/Ru/C as catalysts and the average voltage increment rate was measured to be 0.71 mV/h. The durability of AEMWE was reduced when using non precious metal catalysts (Figs. S11 and S12 in ESI), which could be attributed to the stability and compatibility of electrocatalysts and interfaces.[2,56]

https://doi.org/10.1007/s10118-024-3225-2

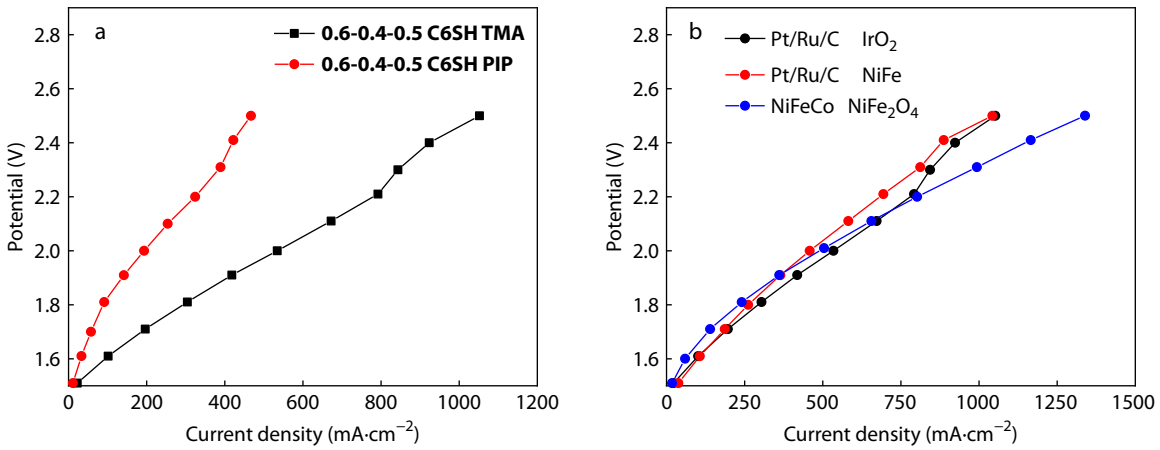

Fig. 6 (a) Polarization curves of **0.6-0.4-0.5 C6SH TMA** and **0.6-0.4-0.5 C6SH PIP** in 1 mol/L KOH at 60 °C of the water electrolyzer; (b) Polarization curves of **0.6-0.4-0.5 C6SH TMA** in 1 mol/L KOH at 60 °C of the water electrolyzer with different anode and cathode catalysts.

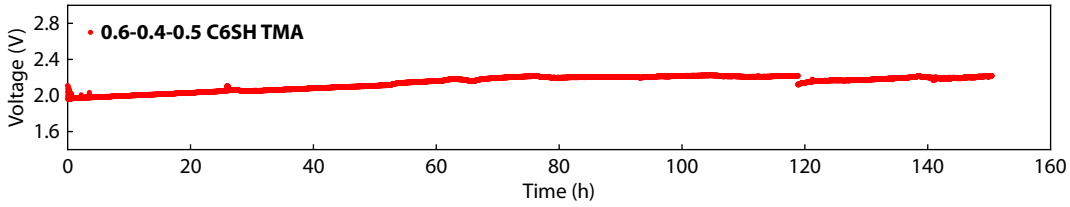

Fig. 7 Durability test of **0.6-0.4-0.5 C6SH TMA** operation at 60 °C in 1 mol/L KOH aqueous solution with catalysts Pt/Ru/C and IrO_2 using a galvanic mode of 500 mA·cm^{-2}.

CONCLUSIONS

In this study, we prepared a series of vinylic-addition polynorbornene-based s-IPN AEMs with poly(5-vinyl-2-norbornene) as the mechanical support phase and a diallylphenol quaternary ammonium salt as the ion conduction phase, cross-linked with various dithiols to obtain interpenetrating polymer networks under UV irradiation by thiol-ene click reaction. This convenient strategy does not need the synthesis of complicated alkyl-substituted norbornene or its corresponding ammonium-functionalized norbornene monomers. The structural effects of cations and dithiols on the performance of s-IPN AEMs were investigated. Under the same feeding ratio, the use of 1,6-hexanedithiol as the cross-linking agent gave rise to the optimal conductivity performance. The hydroxide conductivity of **0.6-0.4-0.5 C6SH TMA** membrane was up to 120 mS/cm at 90 °C. The membranes **0.6-0.4-0.5 C6SH TMA** and **0.6-0.4-0.5 C6SH PIP** exhibited good alkaline stability in 1 M KOH at 80 °C for 35 days. The s-IPN AEMs were successfully applied in alkaline anion-exchange membrane water electrolyzers and operated stably for over 150 h.

Conflict of Interests

The authors declare no interest conflict.

Electronic Supplementary Information

Electronic supplementary information (ESI) is available free of charge in the online version of this article at http://doi.org/10.1007/s10118-024-3225-2.

Data Availability Statement

The data that support the findings of this study are available from the corresponding author upon reasonable request. The author's contact information: weiyou@iccas.ac.cn.

ACKNOWLEDGMENTS

This work was financially supported by the Ministry of Science and Technology of China under the National Key R&D Program of China (No. 2023YFB3811200) and the National Natural Science Foundation of China (No. 22075292).

REFERENCES

1 Du, N.; Roy, C.; Peach, R.; Turnbull, M.; Thiele, S.; Bock, C. Anion-exchange membrane water electrolyzers. *Chem. Rev.* **2022**, *122*, 11830–11895.

2 Yang, Y.; Peltier, C. R.; Zeng, R.; Schimmenti, R.; Li, Q.; Huang, X.; Yan, Z.; Potsi, G.; Selhorst, R.; Lu, X.; Xu, W.; Tader, M.; Soudackov, A. V.; Zhang, H.; Krumov, M.; Murray, E.; Xu, P.; Hitt, J.; Xu, L.; Ko, H. Y.; Ernst, B. G.; Bundschu, C.; Luo, A.; Markovich, D.; Hu, M.; He, C.; Wang, H.; Fang, J.; DiStasio, R. A., Jr.; Kourkoutis, L. F.; Singer, A.; Noonan, K. J. T.; Xiao, L.; Zhuang, L.; Pivovar, B. S.; Zelenay, P.; Herrero, E.; Feliu, J. M.; Suntivich, J.; Giannelis, E. P.; Hammes-Schiffer, S.; Arias, T.; Mavrikakis, M.; Mallouk, T. E.; Brock, J. D.; Muller, D. A.; DiSalvo, F. J.; Coates, G. W.; Abruna, H. D. Electrocatalysis in alkaline media and alkaline membrane-based energy technologies. *Chem. Rev.* **2022**, *122*, 6117–6321.

3 Yang, Y.; Li, P.; Zheng, X.; Sun, W.; Dou, S. X.; Ma, T.; Pan, H. Anion-exchange membrane water electrolyzers and fuel cells. *Chem. Soc. Rev.* **2022**, *51*, 9620–9693.

4 Park, E. J.; Arges, C. G.; Xu, H.; Kim, Y. S. Membrane strategies for water electrolysis. *ACS Energy Lett.* **2022**, *7*, 3447–3457.
5 Santoro, C.; Lavacchi, A.; Mustarelli, P.; Di Noto, V.; Elbaz, L.; Dekel, D. R.; Jaouen, F. What is next in anion-exchange membrane water electrolyzers? Bottlenecks, benefits, and future. *ChemSusChem* **2022,** *15*, e202200027|1–17.
6 Wan, L.; Xu, Z.; Xu, Q.; Pang, M. B.; Lin, D. C.; Liu, J.; Wang, B. G. Key components and design strategy of the membrane electrode assembly for alkaline water electrolysis. *Energy Environ. Sci.* **2023**, *16*, 1384–1430.
7 Varcoe, J. R.; Atanassov, P.; Dekel, D. R.; Herring, A. M.; Hickner, M. A.; Kohl, P. A.; Kucernak, A. R.; Mustain, W. E.; Nijmeijer, K.; Scott, K.; Xu, T. W.; Zhuang, L. Anion-exchange membranes in electrochemical energy systems. *Energy Environ. Sci.* **2014**, *7*, 3135–3191.
8 Chen, N.; Lee, Y. M. Anion exchange polyelectrolytes for membranes and ionomers. *Prog. Polym. Sci.* **2021**, *113*, 101345.
9 You, W.; Noonan, K. J. T.; Coates, G. W. Alkaline-stable anion exchange membranes: a review of synthetic approaches. *Prog. Polym. Sci.* **2020**, *100*, 101177.
10 Nie, G. H.; Wu, W. J.; Yue, X.; Liao, S. J.; Li, X. H. Synthesis and properties of hydroxide conductive polymers carrying dense aromatic side-chain quaternary ammonium groups. *Chinese J. Polym. Sci.* **2017**, *35*, 823–836.
11 Pan, Y.; Wang, T. Y.; Yan, X. M.; Xu, X. W.; Zhang, Q. D.; Zhao, B. L.; El Hamouti, I.; Hao, C.; He, G. H. Benzimidazolium functionalized polysulfone-based anion exchange membranes with improved alkaline stability. *Chinese J. Polym. Sci.* **2017**, *36*, 129–138.
12 Xiong, L.; Hu, Y. F.; Zheng, Z. G.; Xie, Z. L.; Chen, D. Y. Chloromethylation and quaternization of poly(aryl ether ketone sulfone)s with clustered electron-rich phenyl groups for anion exchange membranes. *Chinese J. Polym. Sci.* **2019**, *38*, 278–287.
13 Liu, M.; Hu, X.; Hu, B.; Liu, L.; Li, N. Soluble poly(aryl piperidinium) with extended aromatic segments as anion exchange membranes for alkaline fuel cells and water electrolysis. *J. Membr. Sci.* **2022**, *642*, 119966.
14 Chu, X.; Shi, Y.; Liu, L.; Huang, Y.; Li, N. Piperidinium-functionalized anion exchange membranes and their application in alkaline fuel cells and water electrolysis. *J. Mater. Chem. A* **2019**, *7*, 7717–7727.
15 Cao, D. F.; Yang, F.; Sheng, W. B.; Zhou, Y. F.; Zhou, X. X.; Lu, Y. G.; Nie, F. M.; Li, N. W.; Pan, L.; Li, Y. S. Polynorbornene-based anion exchange membranes with hydrophobic large steric hindrance arylene substituent. *J. Membr. Sci*. **2022,** *641*, 119938.
16 Chen, N.; Hu, C.; Wang, H. H.; Kim, S. P.; Kim, H. M.; Lee, W. H.; Bae, J. Y.; Park, J. H.; Lee, Y. M. Poly(alkyl-terphenyl piperidinium) ionomers and membranes with an outstanding alkaline-membrane fuel-cell performance of 2.58 W cm^{-2}. *Angew. Chem. Int. Ed.* **2021**, *60*, 7710–7718.
17 Wu, X. Y.; Chen, N. J.; Klok, H. A.; Lee, Y. M.; Hu, X. L. Branched poly(aryl piperidinium) membranes for anion-exchange membrane fuel cells. *Angew. Chem. Int. Ed*. **2022,** *61*, e202114892|1–8.
18 Chen, N.; Wang, H. H.; Kim, S. P.; Kim, H. M.; Lee, W. H.; Hu, C.; Bae, J. Y.; Sim, E. S.; Chung, Y. C.; Jang, J. H.; Yoo, S. J.; Zhuang, Y.; Lee, Y. M. Poly(fluorenyl aryl piperidinium) membranes and ionomers for anion exchange membrane fuel cells. *Nat. Commun*. **2021,** *12*, 2367|1–12.
19 Wang, J.; Zhao, Y.; Setzler, B. P.; Rojas-Carbonell, S.; Ben Yehuda, C.; Amel, A.; Page, M.; Wang, L.; Hu, K.; Shi, L.; Gottesfeld, S.; Xu, B.; Yan, Y. Poly(aryl piperidinium) membranes and ionomers for hydroxide exchange membrane fuel cells. *Nat. Energy* **2019**, *4*, 392–398.
20 Olsson, J. S.; Pham, T. H.; Jannasch, P. Poly(arylene piperidinium) hydroxide ion exchange membranes: synthesis, alkaline stability, and conductivity. *Adv. Funct. Mater.* **2018**, *28*, 1702758.
21 Wang, T.; Zhang, Y.; Wang, Y.; You, W. Transition-metal-free preparation of polyethylene-based anion exchange membranes from commercial EVA. *Polymer* **2022**, *262*, 125439.
22 Wang, T.; Wang, Y.; You, W. Dithiol cross-linked polynorbornene-based anion-exchange membranes with high hydroxide conductivity and alkaline stability. *J. Membr. Sci.* **2023**, *685*, 121916.
23 Wang, T.; Wang, Y.; You, W. Polycyclic norbornene based anion-exchange membranes with high ionic conductivity and chemical stability. *J. Membr. Sci.* **2024,** *702*, 122747|1–10.
24 Zhang, F.; Li, T.; Chen, W.; Yan, X.; Wu, X.; Jiang, X.; Zhang, Y.; Wang, X.; He, G. High-Performance Anion Exchange Membranes with Para-Type Cations on Electron-Withdrawing C═O Links Free Backbone. *Macromolecules* **2020**, *53*, 10988–10997.
25 Kwasny, M. T.; Zhu, L.; Hickner, M. A.; Tew, G. N. Thermodynamics of counterion release is critical for anion exchange membrane conductivity. *J. Am. Chem. Soc.* **2018**, *140*, 7961–7969.
26 Zeng, M.; He, X.; Wen, J.; Zhang, G.; Zhang, H.; Feng, H.; Qian, Y.; Li, M. N-methylquinuclidinium-based anion exchange membrane with ultrahigh alkaline stability. *Adv. Mater.* **2023**, *35*, 2306675.
27 Zhang, H.; Wang, X.; Wang, Y.; Zhang, Y.; Zhang, W.; You, W. Alkaline-stable anion-exchange membranes with barium [2.2.2]cryptate cations: the importance of high binding constants. *Angew. Chem. Int. Ed.* **2023**, *62*, e202217742.
28 Wang, W.; Cao, D. F.; Sun, X. W.; Pan, L.; Ma, Z.; Li, Y. S. The influence of various cationic group on polynorbornene based anion exchange membranes with hydrophobic large steric hindrance arylene substituent. *Chinese J. Polym. Sci.* **2022**, *41*, 278–287.
29 Ge, X.; He, Y.; Guiver, M. D.; Wu, L.; Ran, J.; Yang, Z.; Xu, T. Alkaline anion-exchange membranes containing mobile ion shuttles. *Adv. Mater.* **2016**, *28*, 3467–3472.
30 Zhu, Y.; Ding, L.; Liang, X.; Shehzad, M. A.; Wang, L.; Ge, X.; He, Y.; Wu, L.; Varcoe, J. R.; Xu, T. Beneficial use of rotatable-spacer side-chains in alkaline anion exchange membranes for fuel cells. *Energy Environ. Sci.* **2018**, *11*, 3472–3479.
31 Zhang, J.; Zhang, K.; Liang, X.; Yu, W.; Ge, X.; Shehzad, M. A.; Ge, Z.; Yang, Z.; Wu, L.; Xu, T. Self-aggregating cationic-chains enable alkaline stable ion-conducting channels for anion-exchange membrane fuel cells. *J. Mater. Chem. A* **2021**, *9*, 327–337.
32 Yu, W.; Zhang, J.; Liang, X.; Ge, X.; Wei, C.; Ge, Z.; Zhang, K.; Li, G.; Song, W.; Shehzad, M. A.; Wu, L.; Xu, T. Anion exchange membranes with fast ion transport channels driven by cation-dipole interactions for alkaline fuel cells. *J. Membr. Sci.* **2021**, *634*, 119404.
33 Ma, L.; Hussain, M.; Li, L.; Qaisrani, N. A.; Bai, L.; Jia, Y.; Yan, X.; Zhang, F.; He, G. Octopus-like side chain grafted poly(arylene piperidinium) membranes for fuel cell application. *J. Membr. Sci.* **2021**, *636*, 119529.
34 Jeon, S.; Han, S.; Lee, J.; Min, K.; Nam, S. Y.; Kim, T. H. Crosslinked high-performance anion exchange membranes based on poly(dibenzyl -methyl piperidine) and pentafluorobenzoyl-substituted SEBS. *J. Mater. Chem. A* **2024**, *12*, 18593–18603.
35 Lee, Y.; Min, K.; Choi, J.; Choi, G.; Kim, H.; Kim, T. H. Development of highly conductive anion exchange membranes based on crosslinked PIM-SEBS with high free volume. *J. Mater. Chem. A* **2023**, *11*, 25008–25019.
36 Min, K.; Jeong, I.; Kim, H.; Kim, T. H. Polycarbazole-SEBS-crosslinked AEMs based on two spacer polymers for high-performance AEMWE. *J. Mater. Chem. A* **2023**, *12*, 343–353.
37 Guo, D.; Zhuo, Y. Z.; Lai, A. N.; Zhang, Q. G.; Zhu, A. M.; Liu, Q. L. Interpenetrating anion exchange membranes using poly(1-vinylimidazole) as bifunctional crosslinker for fuel cells. *J. Membr. Sci.* **2016**, *518*, 295–304.

https://doi.org/10.1007/s10118-024-3225-2

38 Pan, J.; Zhu, L.; Han, J.; Hickner, M. A. Mechanically tough and chemically stable anion exchange membranes from rigid-flexible semi-interpenetrating networks. *Chem. Mater.* **2015**, *27*, 6689–6698.

39 Zeng, L.; Liao, Y.; Wang, J.; Wei, Z. Construction of highly efficient ion channel within anion exchange membrane based on interpenetrating polymer network for H_2/Air (CO_2-free) alkaline fuel cell. *J. Power Sources* **2021,** *486*, 229377.

40 Zeng, L. P.; Yuan, W.; He, Q.; Ma, X. Q.; Zhang, L.; Wang, J. C.; Wei, Z. D. Dual-Cation interpenetrating polymer network anion exchange membrane for fuel cells and water electrolyzers. *Macromolecules* **2022**, *55*, 4647–4655.

41 Han, J.; Liu, C.; Deng, C.; Zhang, Y.; Song, W.; Zheng, X.; Liu, X.; Zhang, Y.; Yang, X.; Ren, Z.; Hu, M.; Xiao, L.; Zhuang, L. Mechanically robust and highly conductive semi-interpenetrating network anion exchange membranes for fuel cell applications. *J. Power Sources* **2022**, *548*, 232097.

42 Xue, J.; Liu, L.; Liao, J.; Shen, Y.; Li, N. Semi-interpenetrating polymer networks by azide–alkyne cycloaddition as novel anion exchange membranes. *J. Mater. Chem. A* **2018**, *6*, 11317–11326.

43 Matanovic, I.; Maurya, S.; Park, E. J.; Jeon, J. Y.; Bae, C.; Kim, Y. S. Adsorption of polyaromatic backbone impacts the performance of anion exchange membrane fuel cells. *Chem. Mater.* **2019**, *31*, 4195–4204.

44 Mandal, M.; Huang, G.; Kohl, P. A. Highly conductive anion-exchange membranes based on cross-linked poly(norbornene): vinyl addition polymerization. *ACS Appl. Energy Mater.* **2019**, *2*, 2447–2457.

45 Gaitor, J. C.; Yang-Neyerlin, A. C.; Markovich, D.; Fors, B. P.; Coates, G. W.; Kourkoutis, L. F.; Pivovar, B. S.; Kowalewski, T.; Noonan, K. J. T. Comparing ammonium and tetraaminophosphonium anion-exchange membranes derived from vinyl-addition polynorbornene copolymers. *ACS Appl. Energy Mater.* **2024**, *7*, 1517–1526.

46 Mandal, M.; Huang, G.; Kohl, P. A. Anionic multiblock copolymer membrane based on vinyl addition polymerization of norbornenes: applications in anion-exchange membrane fuel cells. *J. Membr. Sci.* **2019,** *570–571*, 394–402.

47 Xie, Y.; Wang, G.; Tang, H.; Wang, G.; Xiao, L.; Zhuang, L. An efficient approach towards highly chemically stable poly(norbornene) membrane for alkaline polyelectrolyte fuel cells. *J. Membr. Sci.* **2024**, *709*, 123057.

48 Zhegur-Khais, A.; Kubannek, F.; Krewer, U.; Dekel, D. R. Measuring the true hydroxide conductivity of anion exchange membranes. *J. Membr. Sci.* **2020**, *612*, 118461.

49 Ziv, N.; Dekel, D. R. A practical method for measuring the true hydroxide conductivity of anion exchange membranes. *Electrochem. Commun.* **2018**, *88*, 109–113.

50 Zhu, M.; Su, Y.; Wu, Y.; Zhang, M.; Wang, Y.; Chen, Q.; Li, N. Synthesis and properties of quaternized polyolefins with bulky poly(4-phenyl-1-butene) moieties as anion exchange membranes. *J. Membr. Sci.* **2017**, *541*, 244–252.

51 Ma, Y.; Hu, C.; Yi, G.; Jiang, Z.; Su, X.; Liu, Q.; Lee, J. Y.; Lee, S. Y.; Lee, Y. M.; Zhang, Q. Durable multiblock poly(biphenyl alkylene) anion exchange membranes with microphase separation for hydrogen energy conversion. *Angew. Chem. Int. Ed.* **2023**, *62*, e202311509.

52 Mohanty, A. D.; Bae, C. Mechanistic analysis of ammonium cation stability for alkaline exchange membrane fuel cells. *J. Mater. Chem. A* **2014**, *2*, 17314–17320.

53 Peltier, C. R.; You, W.; Fackovic Volcanjk, D.; Li, Q.; Macbeth, A. J.; Abruña, H. D.; Coates, G. W. Quaternary ammonium-functionalized polyethylene-based anion exchange membranes: balancing performance and stability. *ACS Energy Lett.* **2023**, *8*, 2365–2372.

54 Hsu, J. H.; Peltier, C. R.; Treichel, M.; Gaitor, J. C.; Li, Q.; Girbau, R.; Macbeth, A. J.; Abruna, H. D.; Noonan, K. J. T.; Coates, G. W.; Fors, B. P. Direct insertion polymerization of ionic monomers: rapid production of anion exchange membranes. *Angew. Chem. Int. Ed.* **2023**, *62*, e202304778.

55 Dang, H. S.; Jannasch, P. A comparative study of anion-exchange membranes tethered with different hetero-cycloaliphatic quaternary ammonium hydroxides. *J. Mater. Chem. A* **2017**, *5*, 21965–21978.

56 Li, D.; Motz, A. R.; Bae, C.; Fujimoto, C.; Yang, G.; Zhang, F. Y.; Ayers, K. E.; Kim, Y. S. Durability of anion exchange membrane water electrolyzers. *Energy Environ. Sci.* **2021**, *14*, 3393–3419.

https://doi.org/10.1007/s10118-024-3225-2